

ORIGINAL ARTICLE

Dispersion and properties of zirconia suspensions for stereolithography

Xingbang Li^{1,2}  | He Zhong¹ | Jingxian Zhang^{1,3} | Yusen Duan^{1,2}  | Hainan Bai^{1,2} | Jingjing Li^{1,2} | Dongliang Jiang¹

¹State Key Laboratory of High Performance Ceramics and Superfine Microstructure, Shanghai Institute of Ceramics, Chinese Academy of Sciences, Shanghai, China

²University of Chinese Academy of Sciences, Beijing, China

³Suzhou Institute of ICCAS (Shanghai Institute of Ceramics, Chinese Academy of Sciences), Taicang, China

Correspondence

Jingxian Zhang, State Key Laboratory of High Performance Ceramics and Superfine Microstructure, Shanghai Institute of Ceramics, Chinese Academy of Sciences, Shanghai 200050, China.
Email: jxzhang@mail.sic.ac.cn

Funding information

National Key Research and Development Program of China, Grant/Award Number: 2017YFB0310400; Research and Development, Grant/Award Number: 2017YFB0310400; National Natural Science Foundation of China, Grant/Award Number: 51572277 51702340; Shanghai Science and Technology Committee; Chinese Academy of Sciences

Abstract

Stereolithography is an attractive technique for the fabrication of complex-shaped ceramic components with high dimensional accuracy. One of the challenges in this technology is the development of high solid loading, low viscosity photosensitive ceramic suspension. In this study, the dispersion of zirconia in photocurable resin and the slurry properties were intensively investigated. Rheological measurements showed that DISPERBYK-103 proved to be an effective dispersant. 42 vol% ZrO₂ suspension was successfully prepared using 3.5 wt% DISPERBYK-103 as the dispersant, with a suitable viscosity (4.88 Pa·s) below the maximum allowable viscosity value (5 Pa·s) for stereolithography applications. The adsorption behavior of DISPERBYK-103 on the surface of zirconia powders was characterized by TG and FT-IR, confirming the dispersion effect of dispersant. Contact angle measurements were also conducted to show that the adsorption of DISPERBYK-103 could help to improve the wettability between powder and photocurable resin. Results showed that DISPERBYK-103 was effective for the preparation of suitable slurries for the development of ZrO₂ ceramics through stereolithography.

KEYWORDS

additive manufacturing, dispersion, stereolithography, suspensions, ZrO₂

1 | INTRODUCTION

Advanced ceramic materials, because of their striking performance such as good mechanical strength, high hardness, excellent corrosion, and high-temperature resistance, have been widely used in many fields ranging from aerospace and medical to ecology and energy.^{1–3} As one of the typical structural ceramics, zirconia ceramics (ZrO₂) distinguish themselves from other ceramic materials due to their unique phase transformation toughening, high temperature ionic conductivity, outstanding biocompatibility, and chemical stability. These advantages have made ZrO₂ an ideal material for dental

implants, oxygen sensors, thermal barrier coatings, and solid oxide fuel cells etc.^{3–5} Nevertheless, it is difficult to fabricate complex-shaped ceramic components by the widely used conventional ceramic shaping processes, unless via the use of special molds. Furthermore, it is known to all that the high cost for producing molds is also one of the constraints for the widespread application of high-tech ceramic materials. Thus, new mold-free technologies would be more challengeable for the widespread application of high-tech ceramic materials.

Ceramic stereolithography is a slurry-based additive manufacturing technique which can directly fabricate high-precision parts layer by layer, without the use of molds or tooling.⁶

The materials used are the blends of photocurable resin and ceramic powders, which can be solidified under a certain amount of radiation. The matrix solution usually consists of several constituents as follows: (a) Monomers. Due to their high photopolymerizable reactivity and conversion, various kinds of acrylates are widely chosen as photocurable monomers and oligomers.⁷ (b) A photoinitiator. The absorptivity of photoinitiator should be tuned to match with the ultraviolet or visible light wavelength, so that it can generate free radicals to initiate the polymerization of the monomer system.^{8,9} (c) Diluents. To control the viscosity of the system, reactive or nonreactive diluents can be added into the slurry. (d) A dispersant, which acts by electrostatic and/or steric repulsion, can also be used to ensure appropriate viscosity and rheological behavior of the high solid loading suspension.¹⁰ In order to reduce shrinkage and avoid cracks which may occur during the elevated temperature heat treatment as well as get a dense sintered body, the solid loading of the slurry should be as high as possible (no less than 40 vol%).¹¹ Nevertheless, it is obvious that the higher the solid loading, the more viscous the slurry. Licciulli et al¹² pointed out that the viscosity of the ceramic suspension for stereolithography should be no more than 5 Pa·s at a shear rate of 30 s⁻¹, to ensure a satisfactory layer recoating via a specific scraper.

For the stereolithography process, the preparation of slurries is the crucial step. Different from the traditional ceramic colloidal processing, stereolithography technique mostly uses low polar acrylate oligomers and monomers as the media. Although there are some works on the stereolithography of zirconia ceramic parts, it is still not well understood for the dispersion and properties of the photocurable zirconia slurries at present. He et al¹³ fabricated zirconia cutting tool and honeycomb component using a DLP stereolithography-based 3D printing. The relative density of the sintered bodies could reach 97.14%, but the significant shrinkage also occurred after debinding and sintering due to the low solid phase content. Sokolov et al¹⁴ investigated the rheological properties of m-ZrO₂ and yttria-stabilized zirconia suspensions based on different (meth)acrylates as organic phase. All the suspensions exhibited pseudoplastic behavior when the solid content was below 32 vol%. However, the rheological behavior of highly concentrated slurry was not studied in their works. Some papers reported the stereolithography for manufacturing zirconia ceramics using slurries with a solid loading exceeding 40 vol%, but their emphases were not on the preparation and optimization of photocurable ceramic suspensions.¹⁵⁻¹⁷

The aim of the present study was to investigate the dispersion and rheological behavior of highly loaded zirconia

suspensions for stereolithography, using commercially available powders and photocurable resin. Rheological measurements are selected to evaluate the flow properties of the slurries. The selection and optimization of dispersing agent and the surface modification of powder were intensively investigated.

2 | EXPERIMENTAL PROCEDURE

2.1 | Starting materials

Commercially available 3 mol% yttria-stabilized zirconia powder, TZ-3YS-E (Tosoh Corp., Tokyo, Japan), was used as received without any purification. The specific surface area and particle size distribution of TZ-3YS-E are shown in Table 1, measured using ASAP2010 (Micromeritics, USA) and Mastersizer 3000 (Malvern, Worcestershire, UK), respectively. A commercially available acrylate-based photocurable resin (SP-RC700, SprintRay Inc., USA) was utilized to bind ceramic particles together. This resin in which ceramic particles have to be dispersed is a low-polar mixture, mainly containing epoxy acrylate, acryloylmorpholine (ACMO), and trimethylolpropane triacrylate (TMPTA). The SP-RC700 presents a Newtonian behavior with a low apparent viscosity of about 40 mPa s (measured by using a rotational rheometer) and can be solidified under a certain amount of radiation with wavelength ranging from 355 to 405 nm. Twelve commercial dispersants presenting good miscibility with the photosensitive resin were used in this manuscript to obtain the well-dispersed suspensions (Table 2). No diluent was introduced in this work.

2.2 | Preparation of the photocurable ceramic suspension

As Table 2 shows, the density of dispersant (about 1 g/cm³) is much lower than that of ZrO₂ (6.09 g/cm³), thus 3-4 wt% addition of the dispersant (with regard to the powder weight) can really change the solid loading efficiently. The composition of 42 vol% slurry with 3.5 wt% dispersant DISPERBYK-103 is shown in Table 3 for example.

The ceramic-resin suspensions with defined composition were mixed by the process of ball milling at room temperature. First the photosensitive resin and a certain amount of dispersant were added into a polyethylene bottle and ball milled for 30 minutes to dissolve the dispersant, using YTZ balls (Nikkato Corp., Osaka, Japan) as the media. Then the zirconia powder was added incrementally

Product name	d_{10} (μm)	d_{50} (μm)	d_{90} (μm)	BET (m ² /g)
TZ-3YS-E	0.232	0.630	4.92	7.133

TABLE 1 Basic properties of raw powder

TABLE 2 Basic data of 12 screened dispersants (all from manufacturer's specifications)

Product name	Chemical description	Density (g/cm ³)	Supplier
TEGO Dispers 628	solution of a copolymer with acidic groups	0.98 (20°C)	Evonik
TEGO Dispers 655	modified polyether with groups of high pigment affinity	1.1 (23°C)	Evonik
TEGO Dispers 670	solution of a polyester derivatives	1.049	Evonik
TEGO Dispers 685	modified polyesterderivative	1.098 (25°C)	Evonik
TEGO Dispers 688	polymer solution	1.014 (20°C)	Evonik
TEGO Dispers 690	polyester with pigment affine groups	1.048 (20°C)	Evonik
Variquat CC 42 NS	polypropoxy quaternary ammonium chloride	1.01 (25°C)	Evonik
DISPERBYK-103	solution of a copolymer with filler affinic groups	1.06 (20°C)	BYK Chemie
DISPERBYK-111	copolymer with acidic groups	1.16 (20°C)	BYK Chemie
DISPERBYK-180	alkylolammonium salt of a copolymer with acidic groups	1.075 (20°C)	BYK Chemie
Triton X 100	octylphenol ethoxylate	1.061 (25°C)	Dow
Oleic acid	CH ₃ (CH ₂) ₇ CH = CH(CH ₂) ₇ COOH	0.89	Aladdin

TABLE 3 Typical composition of 42 vol% zirconia suspension with 3.5 wt% dispersant (on the basis of powder weight)

Starting materials	Zirconia powder	DISPERBYK-103	Photocurable resin
Main usage	Filler	Dispersant	Medium (Binder)
Density (g/cm ³)	6.09	1.06	1.05
Mass fraction (wt%)	80.75	2.82	16.43
Volume fraction (vol%)	42	8.45	49.55

for three times at the interval of at least 1 hour. After the last addition of the powder, the suspension was ball milled for at least 24 hours until the homogeneous mixture was developed. In order to study the adsorption effect of dispersant, 42 vol% zirconia slurries with defined amount of dispersant were prepared. After 24 hour homogenization by ball-milling to reach the saturation adsorption, ethanol was added into the slurry and the zirconia powder in the slurry was obtained by centrifuging at 10 000 rpm and drying at 60°C for 24 hour.

2.3 | Thermal processing

The binder removal of the as-printed zirconia samples was conducted based on the TG-DTA data, with a slow heating rate of 1°C/min up to 600°C and held for 1 hour at 220°C, 350°C and 450°C, respectively. Then the parts were sintered at 1500°C for 2 hour using a heating rate of 5°C/min from 600°C to 1500°C, followed by the free cooling.

2.4 | Characterization

The flow behavior of ceramic suspensions was characterized by rheology analysis in this work. All rheological experiments of the freshly prepared zirconia slurries in the absence and presence of different dispersants were conducted at 25°C through a rotational rheometer MCR301 (Anton Paar, Austria). The parallel plate diameter used was 25 mm, and the gap between the plates was 1 mm. The measurements were carried out by ascending shear rate ramps from 0.001 to 1000 s⁻¹ and descending shear rate ramps from 1000 to 0.001 s⁻¹, respectively, with 10 points of data collected at each order of magnitude with a duration of 2 seconds for each testing point.

TG analysis was performed to measure the adsorbed amount of dispersant on the surface of zirconia particle. PY (Frontier 3030S) and GC/MS (QP2010 Ultra) were combined to analyze the molecule fragments of dispersant after pyrolysis. Fourier transform infrared (FT-IR) spectrometer (Nicolet

iZ10, USA) was also used to test the adsorption of dispersant on powder surface. The contact angle of deionized water and photocurable resin on the surface of untreated and treated particles was measured by dynamic contact angle measuring instrument (SL-200KS, China), respectively, to evaluate the modifying effect of the dispersant for TZ-3YS-E powder surface. The determination of bulk density of the green and sintered parts was accomplished by mercury porosimeter AutoPore IV 9510 (Micromeritics, USA) and Archimedes' method respectively. The microstructure of the sample was observed using a field emission scanning electron microscope (FESEM, Magellan-400, FEI Company).

3 | RESULTS AND DISCUSSION

3.1 | Dispersant

To investigate the dispersion behavior of the zirconia particles in highly loaded slurries, zeta potential measurements are usually utilized. However, the zeta potential value of zirconia powder in photocurable resin is generally low, which makes it difficult to evaluate the dispersion effect of low polar resin-based suspensions.¹⁸ As for ceramic colloidal processing, the dispersant has a great influence on the rheological behavior of the slurry. The dispersant usually has a hydrophilic polar group that can interact with the particle surface and a hydrophobic end chain which can provide steric stabilization in the nonpolar media.¹⁹ The rheological curve of 35 vol% slurry without dispersant was compared with that of slurries containing different kinds of dispersants aiming to break down the agglomerates and to reduce the viscosity, using TZ-3YS-E powder as the filler (Figure 1). All dispersants were added to suspensions at the concentration of 3 wt% (with respect to powder mass), respectively. It is worth

mentioning that Triton X-100 was usually used in BaTiO₃ suspensions for stereolithography.^{20,21} However, the viscosity of the dispersion containing Triton X-100 was too high to be measured in this work. As shown in Figure 1, the rheological behavior of suspension with TEGO-690 is similar to that of the suspension without any dispersant, suggesting that TEGO-690 is useless. It is somewhat surprising that the oleic acid, which has proved to be an efficient dispersant for Al₂O₃,^{11,22} exhibits the worst dispersibility for ZrO₂ powder in stereolithography. As can be seen from the above, not all dispersants can effectively reduce the viscosity. This is because different dispersants contain different anchoring head groups and carbon chain lengths, thus can provide different degrees of steric stabilization.

Of the 12 screened dispersants, DISPERBYK-103 and TEGO-685 are very efficient in terms of viscosity decreasing, which can be seen in Figure 1. It is probably due to the anchoring functional groups of them can easily bind to the ZrO₂ particle surface, while their end chains show a good affinity to low-polar media.²³ Figure 2 shows the rheological behaviors of 35 and 42 vol% suspensions with DISPERBYK-103 or TEGO-685 (3 wt% with respect to the total mass of zirconia powder). As expected, the viscosity of the suspension increased as the solid loading increased, under the condition of using the same dispersant with the same adding amount. The viscosities of the two slurries containing DISPERBYK-103 decreased with the increase of shear rate, all showing typical shear-thinning behavior at shear rates ranging from 0.005 to 500 s⁻¹. Shear-thinning behavior is desirable in stereolithography process because it can allow the satisfactory spreading of thin layers and thus can achieve a homogeneous green microstructure.^{9,24} The two suspensions with TEGO-685 exhibited low viscosities and shear-thickening behaviors at very low shear rates, but showed Newtonian fluid performances

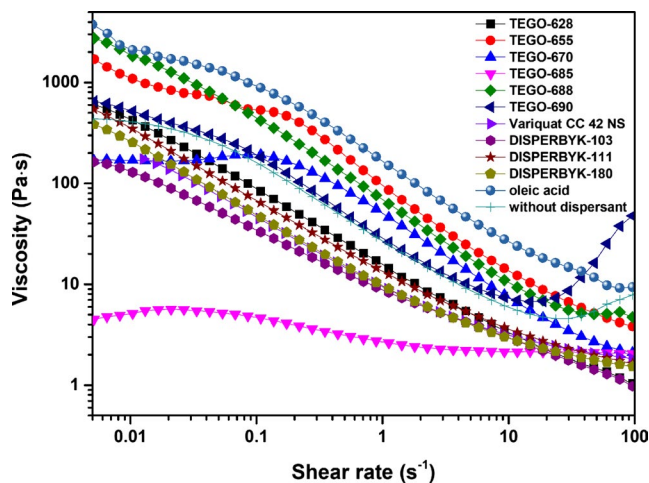


FIGURE 1 Viscosity as a function of shear rate for 35 vol% suspensions with different dispersant (3 wt% with regard to the mass of the powder)

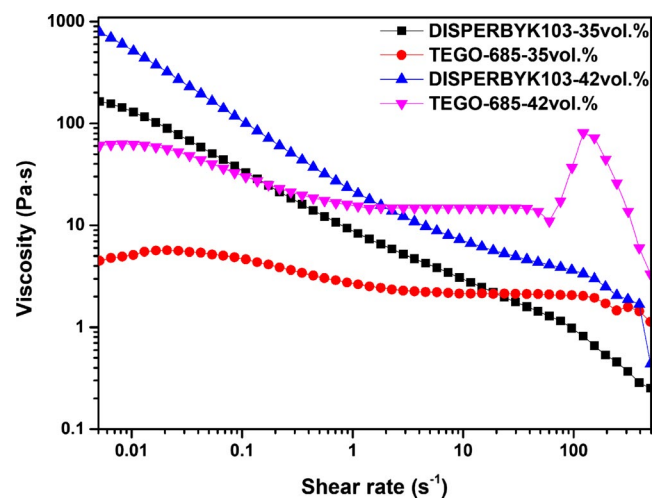


FIGURE 2 Rheological properties of 35 and 42 vol% suspensions with DISPERBYK-103 or TEGO-685 as the dispersant

for the intermediate shear rates. These complicated phenomena might be related to the molecular weight and dosage of TEGO-685 as well as the dispersant/resin interaction, which deserve further research and will not be discussed in detail in this paper.

As can be seen in Figure 2, the viscosity of suspension TEGO-685-42 vol% was higher than that of suspension DISPERBYK-103-42vol.% after the shear rate of 2 s^{-1} , even far exceeds the maximum allowable viscosity value corresponding to $5 \text{ Pa}\cdot\text{s}$. Furthermore, a severe shear-thickening behavior occurred when the shear rate exceeds 60 s^{-1} , suggesting the formation of jamming clusters caused by hydrodynamic lubrication forces.²⁵ This may be due to the high molecular weight of TEGO-685 and high solid loading of slurry. However, during the testing process, this slurry was not stable at high shear rate and led to a sudden drop at high shear rate. This viscosity curve confirmed that the dispersant was not suitable for the dispersion of zirconia in the acrylate-based solution. Considering most of scrapers are set to work at shear rates from 30 to 100 s^{-1} , DISPERBYK-103 is more suitable than TEGO-685 for preparing high solid loading photocurable ZrO_2 slurry.

3.2 | Optimization of dispersant concentration

The optimal dispersant content can also be evaluated through rheological measurements. Figure 3A displayed the rheological behaviors of the 42 vol% zirconia-resin suspensions with different concentration of DISPERBYK-103. As can be seen in this figure, all of the slurries exhibited shear-thinning behaviors, prepared with the incremental amount of dispersant from 2.5 to 4.0 wt% (with respect to the powder weight). The viscosities of suspensions with the minimum 2.5 wt% and the maximum 4.0 wt% of DISPERBYK-103 were much higher than that of other suspensions over the whole shear rate range. Figure 3B illustrated the viscosity values measured under the shear rate of 30 s^{-1} . It can be observed that with the increase of dispersant, the viscosity of the slurry steadily decreased at first, until it reached a minimum and then increased. The addition of 3.5 wt% DISPERBYK-103 led to the least viscosity ($4.88 \text{ Pa}\cdot\text{s}$ at shear rate of 30 s^{-1}) corresponding to the best state of dispersion, below the maximum allowable viscosity value ($5 \text{ Pa}\cdot\text{s}$ at shear rate of 30 s^{-1}) proposed by Licciulli.¹² If the concentration of DISPERBYK-103 is too low, the modifying effect of dispersant to powder is not enough to compensate the Van der Waals attractive forces between particles and to prevent the collision of particles caused by Brownian motion, thus leading to the poor stability and dispersibility of slurries. However, when dispersant concentration exceeds the optimum dose, the free dispersant molecular between the particles increases significantly in the suspension. The excessive free dispersant molecular may

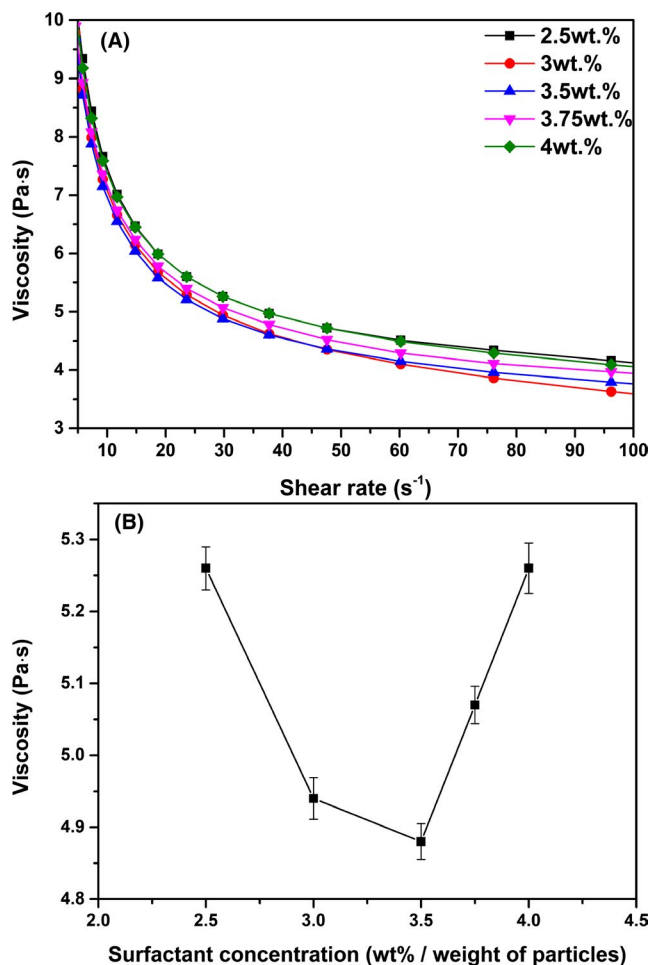


FIGURE 3 Viscosities of 42 vol% solid loading slurries with different dispersant content at shear rates from 5 to 100 s^{-1} (A) and at a shear rate of 30 s^{-1} (B)

introduce unwanted tangles between them, which is known as bridging flocculation especially in highly concentrated suspension. As a consequence, the particle agglomeration and high viscosity would occur after the optimized dispersant concentration.^{11,25}

Figure 4 shows the adsorption quantity of DISPERBYK-103 on the surface of zirconia powders as a function of dispersant concentration. Initially, the adsorption amount increases with the increase of dispersant concentration from 1.0 to 3.5 wt%, suggesting a good affinity of DISPERBYK-103 for the zirconia powder surface. The modifying effect of dispersant to powder can improve the stability of the system and result in a decrease in suspension viscosity,²⁶ corresponding to Figure 3B. Nevertheless, after the minimum viscosity (3.5 wt% dispersant at this time) was reached, the adsorption amount decreased with the increase of dispersant. This phenomenon might be explained by the interaction of the dispersant adsorbed on the powder surface with the excessive dispersant molecular kept in the suspension. In addition, as mentioned

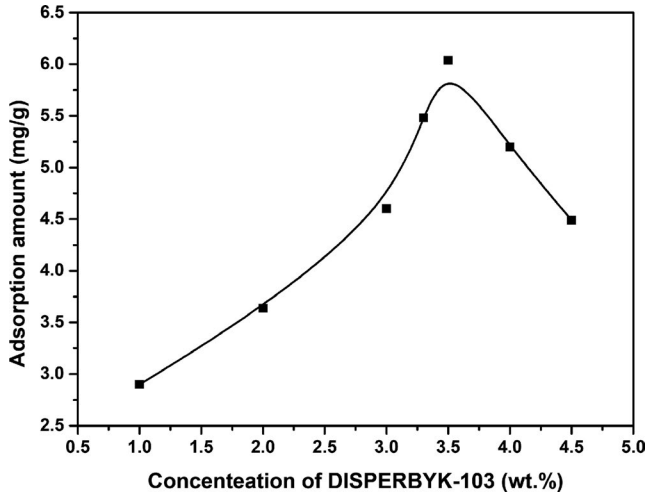


FIGURE 4 Adsorption of DISPERBYK-103 on ZrO_2 particle surface as a function of dispersant content (based on zirconia powder)

above, the particle agglomeration occurred when the dispersant content exceeded its optimum dose, which can also result in the increase in slurry viscosity and the decrease in dispersant adsorption amount.

As a result, the suitable dispersant chosen to ensure the stability of the high solid content ZrO_2 photocurable slurries is DISPERBYK-103, with an optimum concentration set at 3.5 wt% with regard to the powder weight.

3.3 | Surface modification of zirconia particles via DISPERBYK-103

From the Technical Data Sheet (TDS) of DISPERBYK-103, the solvent used is methoxypropylacetate. The active

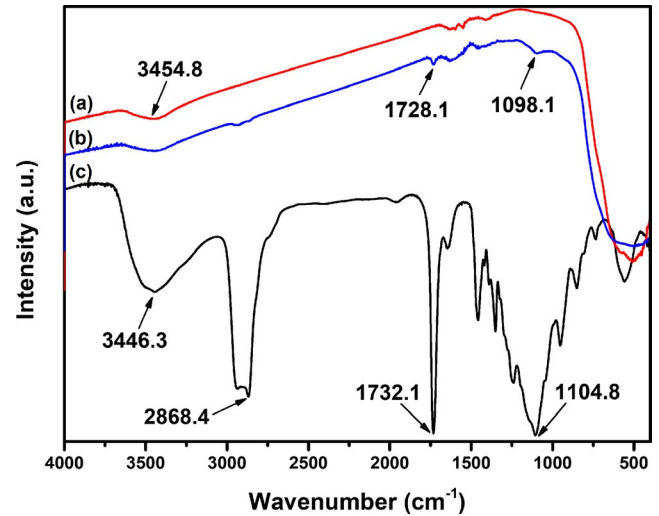
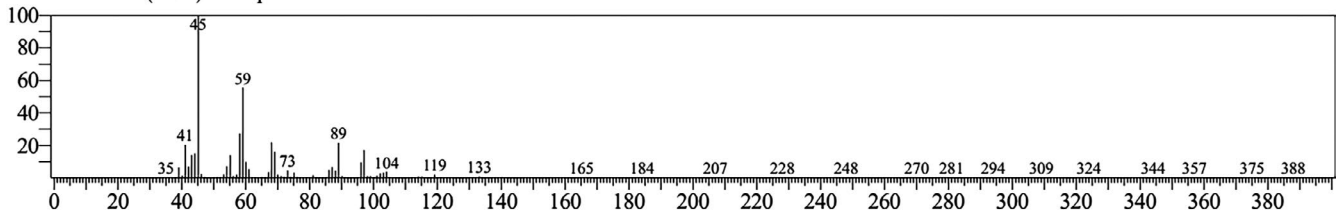


FIGURE 6 FT-IR spectrum of (a) as-received powder, (b) modified powder and (c) DISPERBYK-103

ingredient of DISPERBYK-103 is a copolymer with filler affinic groups (Table 2). One of the polymerized monomers is a modified ethylene oxide (EO), according to PY-GC/MS results (Figure 5). Figure 6A is the FT-IR spectrum of untreated ZrO_2 powder (TZ-3YS-E). The broad band at 3454.8 cm^{-1} is defined as the stretching vibration peak of hydroxy (O-H).^{27,28} It was reported by numerous researches that some oxide powders, such as alumina, silica, and zirconia typically have hydroxy group on their surface which can account for their hydrophilic nature.²² Figure 6C shows the FT-IR spectrum of the active ingredient of DISPERBYK-103. The strong peaks at 1732.1 and 1104.8 cm^{-1} correspond to the

<< Target >>

Line#:12 R.Time:9.003(Scan#:2462) MassPeaks:249
RawMode:Single 9.003(2462) BasePeak:45.10(1927716)
BG Mode:8.770(2392) Group 1 - Event 1 Scan



Hit#:1 Entry:22846 Library:NIST14.lib

SI:80 Formula:C7H16O4 CAS:112-35-6 MolWeight:164 RetIndex:1187

CompName:Ethanol, 2-[2-(2-methoxyethoxy)ethoxy]- \$\$\$\$ Dowanol TMA \$\$\$\$ Methoxytriethylene glycol \$\$\$\$ Methoxytriglycol \$\$\$\$ Methyltrioxitol \$\$\$\$ Triethyl

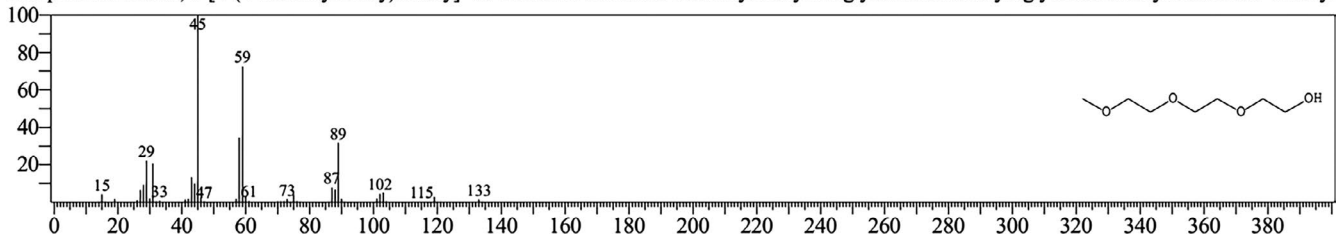


FIGURE 5 Fragment information of modified polyoxyethylene ether from PY-GC/MS of DISPERBYK-103

stretching vibration peaks of C = O and C–O–C, respectively. Figure 6B is the FT-IR spectrum of the powder modified with 3.5 wt% DISPERBYK-103, after centrifuged using ethanol at 10 000 rpm and dried at 60°C for 24 hour. Compared with the spectrum of raw powder, the presence of C = O (1728.1 cm^{-1}) and C–O–C (1098.1 cm^{-1}) shown in Figure 6B proved the adsorption of DISPERBYK-103 on particle surface.

Table 4 and Figure 7 shows the contact angles measured between deionized water, photocurable resin, and untreated

TABLE 4 Contact angle measurements of deionized water and photocurable resin with different zirconia substrates

Substrate	Liquid	Contact angle (°)
Untreated zirconia powder (A)	Deionized water	22.57
Untreated zirconia powder (B)	Photocurable resin	38.61
Modified zirconia powder (C)	Deionized water	34.33
Modified zirconia powder (D)	Photocurable resin	28.21

powder compact also between deionized water, photocurable resin, and powder compact treated with DISPERBYK-103. As shown in Table 4, the contact angle value between zirconia powder and water (A) is smaller than that between zirconia powder and resin (B). This is due to the hydrophilic nature of raw zirconia powder as mentioned above. The powder treated with DISPERBYK-103 owns a better wettability with the hydrophobic photocurable resin by comparing the contact angle of (B) and (D). Hence, the modification of zirconia powder via DISPERBYK-103 might be a kind of hydrophobization and help to increase the affinity of resin with the powder surface, thus lead to the better dispersion behavior.

3.4 | Stereolithography fabrication of zirconia parts

Based on the optimization of the dispersion behavior, well-dispersed ZrO_2 slurries with the solid content as 42 using 3.5 wt% DISPERBYK-103 were prepared for stereolithography. Figure 8 shows the 3D zirconia green parts printed on ADMAFLEX 130, a DLP-based additive manufacturing system that has been developed and commercialized by ADMATEC Europe

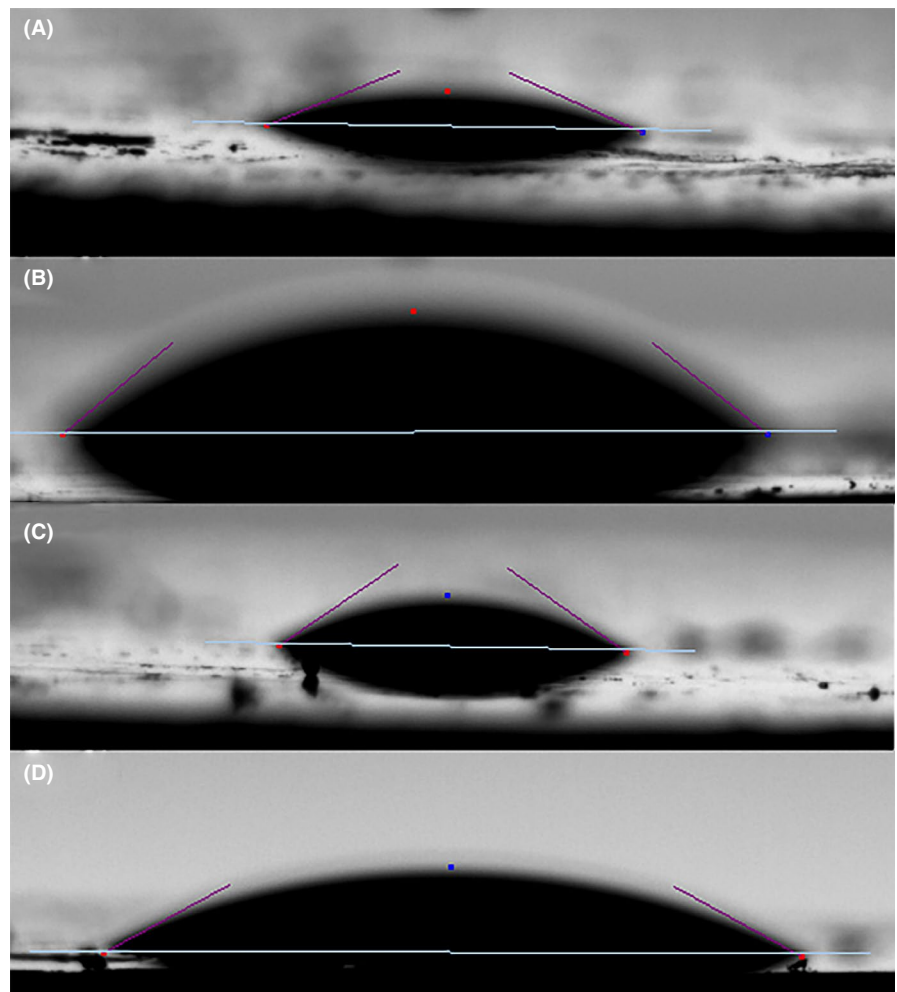


FIGURE 7 Test picture of the contact angles between water and untreated powder (A), resin and untreated powder (B), water and treated powder (C), resin and treated powder (D)

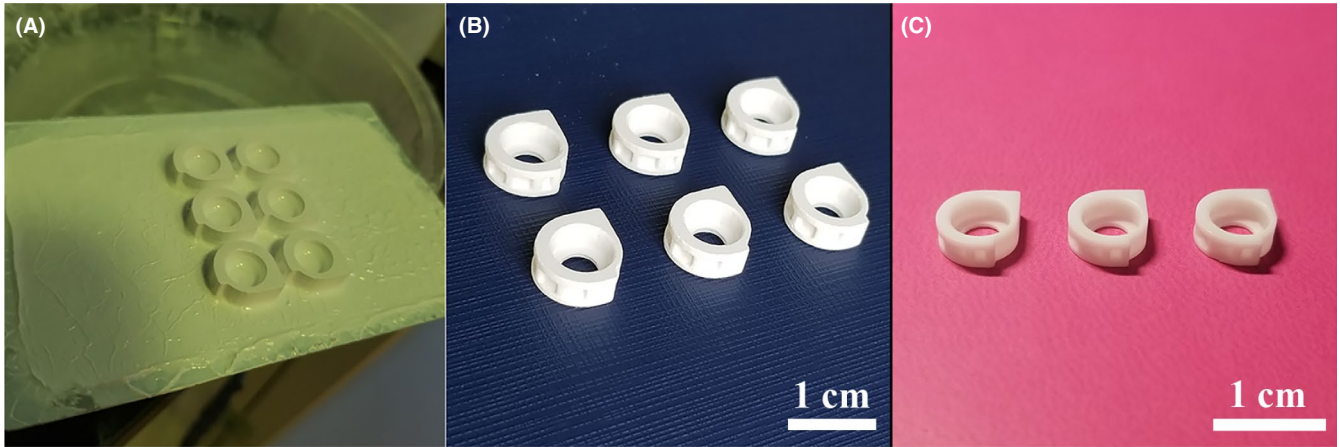


FIGURE 8 Photos of samples: (A) as-printed, (B) after cleaned using ethanol and (C) after sintering

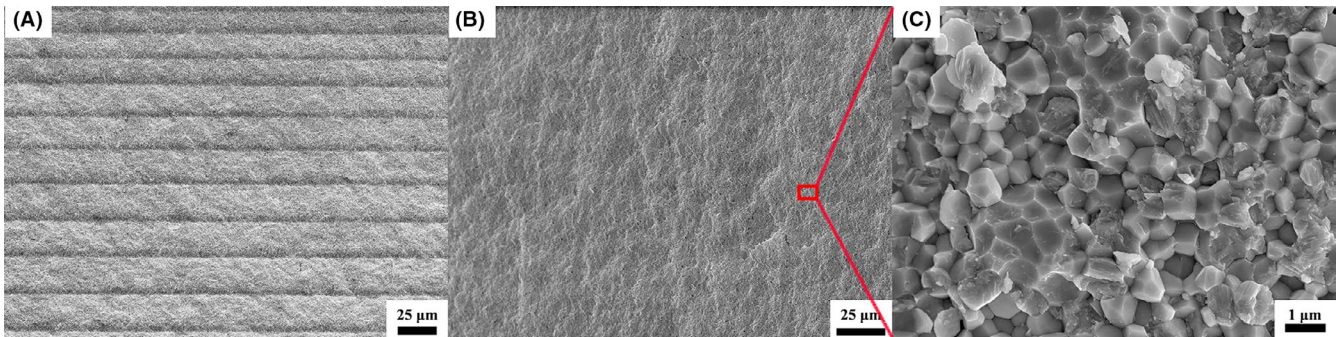


FIGURE 9 Fracture surface SEM micrographs of samples: (A) green body at low magnification; (B) sintered sample at low magnification; (C) sintered sample at high magnification

BV, with the exposure time and layer thickness set as 1.5 s and 25 μm , respectively. Figure 9 shows the SEM micrograph of the fracture surface of the samples. The layered structure with the thickness of about 25 μm can be seen in Figure 9A. This is typical for the DLP-based stereolithography due to its specific production technique route. However, due to the decomposition of most of the polymers during heat-treatment, the ceramic particles tended to stack freely first, and then the densification was achieved progressively with the increase in temperature.²⁹ Thus, the individual layers will be densified together and the “stair steps” disappeared after sintering (Figure 9B). Figure 9C is a SEM micrograph of sintered sample at high magnification taken from Figure 9B, illustrated by a red rectangular box. As Figure 9B and Figure 9C show, there are neither discernible pores nor other defects in the microstructure of the sintered part, which indicates a high level of densification. The linear shrinkage ratios of the parts in the $X(Y)$ and Z directions during heat treatment process were $22.53 \pm 0.04\%$ and $22.63 \pm 0.31\%$, respectively. The 98.02% relative density of sintered body was calculated by Archimedes’ method, suggesting the formed ceramic body with good quality can be obtained by the optimization of slurry properties (Table 5).

TABLE 5 Density and porosity of green and sintered part

	Bulk density (g/cm^3)	Porosity (%)
Green body	3.1080	13.7220
Sintered body	5.9694	1.98

4 | CONCLUSIONS

In this work, the high solid loading (42 vol%) zirconia photocurable dispersions with a low viscosity $< 5 \text{ Pa}\cdot\text{s}$ at 30 s^{-1} shear rate and a representative shear-thinning behavior suitable for stereolithography applications were successfully prepared. Rheological measurements showed that DISPERBYK-103 turned out to be a very effective dispersant, and its optimum addition content was 3.5 wt% on a dry weight basis of ceramic powders by combining the rheology and adsorption amount results. The insufficiency or excess of dispersant can cause the increase in viscosity as well as the drop in adsorption amount on particle surface. FT-IR spectra revealed the presence of carbonyl and ether groups on the surface of modified powder, illustrating the effective modification of

zirconia particle surface. Contact angle measurements indicated that the treated powder showed better wettability with low-polar photosensitive than raw powder. Results showed that the obtained slurry with well dispersed state is suitable for the stereolithography applications.

ACKNOWLEDGMENTS

This work was supported by the National Key Research and Development Program of China (2017YFB0310400), National Natural Science Foundation of China (No. 51572277, 51702340), Shanghai Science and Technology Committee (17YF1428800, 17ZR1434800, 17dz2307000), and the State Key Laboratory of High Performance Ceramics and Superfine Microstructure of Shanghai Institute Ceramics, Chinese Academy of Sciences.

ORCID

Xingbang Li  <https://orcid.org/0000-0001-8000-2951>

Yusen Duan  <https://orcid.org/0000-0002-3750-9295>

REFERENCES

- Belmonte M. Advanced ceramic materials for high temperature applications. *Adv Eng Mater.* 2006;8:693–703.
- Chevalier J, Gremillard L. Ceramics for medical applications: a picture for the next 20 years. *J Eur Ceram Soc.* 2009;29:1245–55.
- Cao XQ, Vassen R, Stoeber D. Ceramic materials for thermal barrier coatings. *J Eur Ceram Soc.* 2004;24:1–10.
- Sillassen M, Eklund P, Pryds N, Johnson E, Helmersson U, Böttiger J. Low-temperature superionic conductivity in strained yttria-stabilized zirconia. *Adv Funct Mater.* 2010;20:2071–6.
- Abd El-Ghany OS, Sherief AH. Zirconia based ceramics, some clinical and biological aspects: review. *Future Dent J.* 2016;2:55–64.
- An D, Li HZ, Xie ZP, Zhu TB, Luo XD, Shen ZJ, et al. Additive manufacturing and characterization of complex Al₂O₃ parts based on a novel stereolithography method. *Int J Appl Ceram Tec.* 2017;14:836–44.
- Schwarzer E, Gotz M, Markova D, Stafford D, Scheithauer U, Moritz T. Lithography-based ceramic manufacturing (LCM) - Viscosity and cleaning as two quality influencing steps in the process chain of printing green parts. *J Eur Ceram Soc.* 2017;37:5329–38.
- Griffith ML, Halloran JW. Freeform fabrication of ceramics via stereolithography. *J Am Ceram Soc.* 1996;79:2469–74.
- Hinczewski C, Corbel S, Chartier T. Ceramic suspensions suitable for stereolithography. *J Eur Ceram Soc.* 1998;18:583–90.
- Hinczewski C, Corbel S, Chartier T. Stereolithography for the fabrication of ceramic three-dimensional parts. *Rapid Prototyping J.* 1998;4:104–11.
- Li KH, Zhao Z. The effect of the surfactants on the formulation of UV-curable SLA alumina suspension. *Ceram Int.* 2017;43:4761–7.
- Licciulli A, Corcione CE, Greco A, Amicarelli V, Maffezzoli A. Laser stereolithography of ZrO₂ toughened Al₂O₃. *J Eur Ceram Soc.* 2005;25:1581–9.
- He R, Liu W, Wu Z, An Di, Huang M, Wu H, et al. Fabrication of complex-shaped zirconia ceramic parts via a DLP-stereolithography-based 3D printing method. *Ceram Int.* 2018;44:3412–6.
- Sokolov PS, Komissarenko DA, Dosovitskii GA, Shmeleva IA, Slyusar' IV, Dosovitskii AE. Rheological properties of zirconium oxide suspensions in acrylate monomers for use in 3D printing. *Glass Ceram.* 2018;75:55–9.
- Mitteramskogler G, Gmeiner R, Felzmann R, Gruber S, Hofstetter C, Stampfl J, et al. Light curing strategies for lithography-based additive manufacturing of customized ceramics. *Addit Manuf.* 2014;1–4:110–8.
- Xing HY, Zou B, Li SS, Fu XS. Study on surface quality, precision and mechanical properties of 3D printed ZrO₂ ceramic components by laser scanning stereolithography. *Ceram Int.* 2017;43:16340–7.
- Harrer W, Schwentenwein M, Lube T, Danzer R. Fractography of zirconia-specimens made using additive manufacturing (LCM) technology. *J Eur Ceram Soc.* 2017;37:4331–8.
- Zhang K, Xie C, Wang G, He R, Ding G, Wang M, et al. High solid loading, low viscosity photosensitive Al₂O₃ slurry for stereolithography based additive manufacturing. *Ceram Int.* 2019;45:203–8.
- Liu J-C, Jean J-H, Li C-C. Dispersion of nano-sized γ -alumina powder in non-polar solvents. *J Am Ceram Soc.* 2006;89:882–7.
- Jang JH, Wang S, Pilgrim SM, Schulze WA. Preparation and characterization of barium titanate suspensions for stereolithography. *J Am Ceram Soc.* 2000;83:1804–6.
- Chen Z, Song X, Lei L, Chen X, Fei C, Chiu CT, et al. 3D printing of piezoelectric element for energy focusing and ultrasonic sensing. *Nano Energy.* 2016;27:78–86.
- Adake CV, Bhargava P, Gandhi P. Effect of surfactant on dispersion of alumina in photopolymerizable monomers and their UV curing behavior for microstereolithography. *Ceram Int.* 2015;41:5301–8.
- Sun J, Binner J, Bai J. Effect of surface treatment on the dispersion of nano zirconia particles in non-aqueous suspensions for stereolithography. *J Eur Ceram Soc.* 2019;39:1660–7.
- Chartier T, Duterte C, Delhote N, Baillargeat D, Verdeyme S, Delage C, et al. Fabrication of millimeter wave components via ceramic stereo- and microstereolithography processes. *J Am Ceram Soc.* 2008;91:2469–74.
- Goswami A, Ankit K, Balashanmugam N, Umarji AM, Madras G. Optimization of rheological properties of photopolymerizable alumina suspensions for ceramic microstereolithography. *Ceram Int.* 2014;40:3655–65.
- Yu M, Zhang J, Li X, Liang H, Zhong He, Li Y, et al. Optimization of the tape casting process for development of high performance alumina ceramics. *Ceram Int.* 2015;41:14845–53.
- Liu W, Xie Z, Yang X, Wu Y, Jia C, Bo T, et al. Surface modification mechanism of stearic acid to zirconia powders induced by ball milling for water-based injection molding. *J Am Ceram Soc.* 2011;94:1327–30.
- Li X, Jiang D, Zhang J, Lin Q, Chen Z, Huang Z. The dispersion of boron carbide powder in aqueous media. *J Eur Ceram Soc.* 2013;33:1655–63.
- Hu S, Liu Y, Zhang Y, Xue Z, Wang Z, Zhou G, et al. 3D printed ceramic phosphor and the photoluminescence property under blue laser excitation. *J Eur Ceram Soc.* 2019;39:2731–8.

How to cite this article: Li X, Zhong H, Zhang J, et al. Dispersion and properties of zirconia suspensions for stereolithography. *Int J Appl Ceram Technol.* 2019;00:1–9. <https://doi.org/10.1111/ijac.13321>